Trends, periodicities and discontinuities of precipitation in the Huangfuchuan Watershed, Loess Plateau, China

Yi He[1], Xingmin Mu[1–3], Peng Gao[2,3,*], Guangju Zhao[2,3], Fei Wang[2,3], Wenyi Sun[2,3], Pengfei Li[3] and Jinxi Song[3]

[1]College of Water Resources and Architectural Engineering, and
[2]Institute of Soil and Water Conservation, Northwest A&F University, Yangling 712100, Shaanxi, China
[3]Institute of Soil and Water Conservation, Chinese Academy of Sciences and Ministry of Water Resources, Yangling 712100, Shaanxi, China

Longitudinal analyses of hydro-meteorological variables are extremely important for climate studies and water resources planning. Precipitation across the most severely eroded areas of Huangfuchuan Watershed in the Loess Plateau, China was analysed using data from 10 rainfall stations during the period 1954–2010. The ensemble empirical mode decomposition (EEMD), Hurst exponent, and Mann–Kendall methods were utilized to detect periodicities, discontinuities as well as long-term persistence of precipitation. The results show abrupt changes (i.e. discontinuities) in spring during the period 1963–1969 and in 1975, the summer period of 1962 and 1986–1994, the autumn of 1978, and the winter of 1964. These abrupt changes were determined to be statistically significant at the $P = 0.05$ level. There were inter-annual periods of quasi-3- and quasi-6-year for annual and the four seasons, and decadal periods of quasi-10-, quasi-15-, quasi-25- and quasi-50-year for different seasons. However, periodical features in inter-annual periods were not statistically noticeable. Moreover, Hurst exponent analysis indicated that the current trends of precipitation over the four seasons would continue in the future. The results also indicate that the EEMD method is able to effectively reveal deviations in long-term precipitation series at various timescales and could be utilized for complex analysis of non-stationary and nonlinear signal change. These findings could provide important information for ecological restoration and farming operations across the study region.

Keywords: Ensemble empirical mode decomposition, periodicities and discontinuities, precipitation variability, watershed.

TIME series analysis of observational hydroclimatic data generates direct information regarding changes in hydrology. Therefore, this type of analysis is extremely important for understanding and managing water resources. Large-scale variations in water-cycle parameters and hydrological variables require further studies to determine their potential impacts on hydrologic hazards and water resources. In this context, precipitation is an important climatic parameter as it directly affects the availability of water resources.

During the last several years, many studies have been conducted that quantify precipitation variation using various approaches and in several different regions. For example, Coulibaly[1] used the cross-wavelet and wavelet methods to identify and describe temporal and spatial variation of seasonal precipitation in Canada. This study provided insights into the dynamic relationship between the dominant modes of climate variation in the northern hemisphere and seasonal precipitation. Li *et al.*[2] evaluated the variation in seasonal and annual precipitation using the Hurst exponent and Mann–Kendall (MK) test methods in Xinjiang, China. Xue *et al.*[3] decomposed the autumn precipitation series in the Weihe River Basin, China, using the ensemble empirical mode decomposition (EEMD) method and determined the precipitation periodicity characteristics at various scales. Deng *et al.*[4] analysed precipitation during summer and spring within the watershed of the Yangtze River, China using the empirical mode decomposition (EMD) method. They showed that there were similar periods of rainfall in these seasons.

The middle reaches of the Yellow River, China, flow through semi-arid and arid regions. However, few studies have investigated the impact of precipitation changes on water resources and hydrology. The Huangfuchuan River is a major tributary of the Yellow River and one of the main sources of coarse sand. Due to sparse vegetation, thick loess that is highly susceptible to erosion, the relatively high intensity of rainstorms, uneven temporal distribution of rainfall and harmful human activities, soil erosion in the Huangfuchuan Watershed, Loess Plateau has caused substantial damage. Rainfall is the main dynamic factor that causes soil loss as its level and intensity can influence the occurrence of soil erosion. This can lead to altered land-use management strategies, agricultural practices and vegetation growth conditions.

The periodicity of precipitation is a characteristic that is often utilized in the analysis of hydrologic time series[5–7]. There have been a significant number of studies on precipitation periodicity that have employed various methods and techniques for the identification of periods[8,9]. However, hydrologic time series typically exhibits non-stationary and nonlinear characteristics[10], and the limitations of these traditional techniques cannot satisfy the requirements of current hydrologic research[5]. In order to improve the identification of periodicity in time series, various novel methodologies have been employed in the hydrological literature. EEMD has widespread use for the analysis of time series data, such as surface temperature[11], tree ring data[12] and changes in the onset of seasons[13].

*For correspondence. (e-mail: gaopeng@ms.iswc.ac.cn)

To date, most of the studies on precipitation variation have focused on annual variation. Furthermore, few studies have been conducted to identify climate change signals via the periodicity of precipitation time series in the Huangfuchuan Watershed. Therefore, the objectives of the present study were to investigate the periodicity characteristics of annual and seasonal precipitation using monthly precipitation datasets during 1954–2010, to explore future trends in seasonal and annual precipitation via the Hurst exponent method and to evaluate abrupt changes in annual and seasonal precipitation.

The Huangfuchuan Watershed is situated in the northern area of the Yellow River Basin within 110°18′–11°12′E and 39°12′–39°54′N. The Huangfuchuan River has a length of 137 km and the watershed area is 3246 km^2. The annual precipitation is 350–450 mm, and >80% of the precipitation falls during the period June–September. Vegetation in this area has been largely destroyed. The removal of vegetation, in conjunction with the large terrain height difference and strong rainfall, has caused severe soil and water loss. The area introduces approximately 0.15×10^9 tonnes of sediment into the Yellow River each year. This has led to devastating impacts on the ecological communities and agriculture conditions (Figure 1)[14].

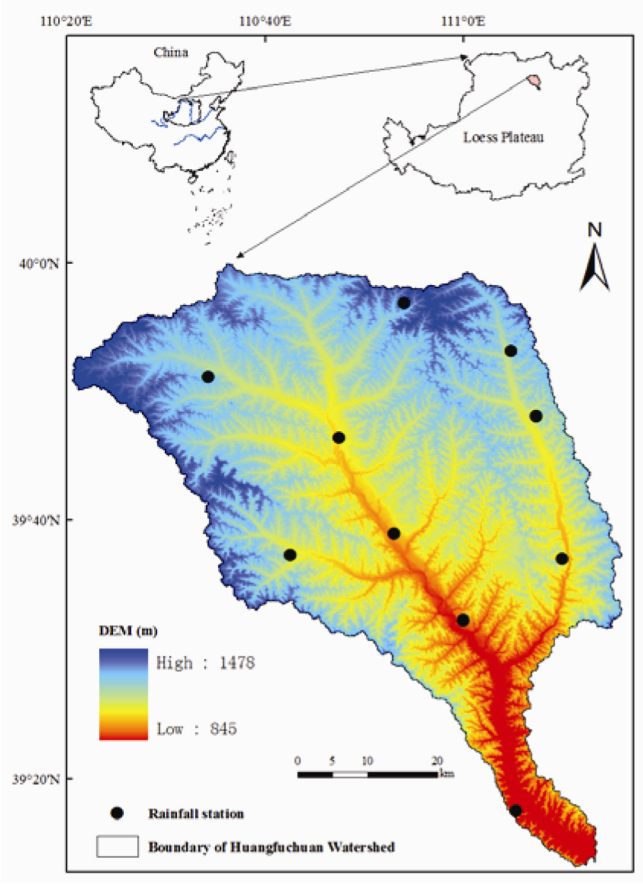

Figure 1. Map of the study region.

Rainfall data from 10 stations were analysed in this study (Figure 1), including annual precipitation and monthly precipitation during 1954–2010. Considering the hydrogeology conditions of the study area and the fact that the distribution of precipitation in the rainy season is the driving force for soil erosion, we defined winter as December–February, spring as March–May, summer as June–August and autumn as September–November.

MK is a non-parametric statistical test that has been frequently used to determine the significance of patterns in hydro-meteorological time series[15,16]. For more details on the MK test, readers may refer to Zhang *et al.*[17]. Here, we employ the MK test for studying annual and seasonal trends and to identify abrupt changes in precipitation trends within the Huangfuchuan Watershed.

EEMD is a central component of the Hilbert–Huang transformation. It is an adaptive technique that can decompose a time series into intrinsic mode functions (IMFs) and a long-term trend[18]. Each IMF represents a specific frequency range, i.e. from high- to low-frequency modes. The frequency of the IMFs decreases with their order, with the first IMF having the highest frequency. The summation of the long-term trend and these IMFs recreates the original time series. The number of IMFs is dependent on the duration of the time series. The EEMD method improves upon the EMD method[19,20]. The latter is an adaptive method that is able to decompose any complex data series into a finite set of amplitude–frequency-modulated oscillatory components. Additional details regarding EMD and EEMD can be found in Wu and Huang[21]. In this study, we have used 100 as the ensemble number and set the amplitude of added white noise to 0.2 times the standard deviation of data, based on suggestion by Wu and Huang[21].

The Hurst exponent method is used to quantify the long-term memory of the time series, and the Hurst exponent is estimated using range/standard deviation (R/S) analysis. It is a method of time-series analysis that utilizes fractal theory. This technique has widespread use in climate change and geographic research[22]. Here, Hurst exponent analysis is used to study future precipitation trends. The Hurst index (H) has the ability to project future time-series trends according to past trends; it has been used to predict hydrological and climatological processes[2,23]. H ranges between 0 and 1. If (1) $H = 0.50$, it suggests that the various essential elements are entirely independent and the change is random. An H value between 0.50 and 1.00 indicates that the long-term trend of the time series will probably continue in the future. The closer the H value is to 1.00, the stronger the likelihood of this continuation. An H value between 0.00 and 0.50 also suggests that the time series has a long-term trend. However, this value range indicates that the future tendency will be the opposite of the long-term trend. The closer the H value is to 0.00, the higher the likelihood for a reversal of the long-term trend.

Table 1. Statistics for annual and seasonal precipitation within the Huangfuchuan Watershed during 1954–2010

Statistics	P (mm)	P_1 (mm)	P_2 (mm)	P_3 (mm)	P_4 (mm)
Mean	362.0	47.9	235.8	71.1	7.4
Minimum	94.3	1.5	38.6	17.5	0.0
(year)	(1955)	(1955)	(1955)	(1965)	(1954–58)
Maximum	838.1	136.6	732.3	157.1	23.2
(year)	(1959)	(1991)	(1959)	(1960)	(1978)
Median	356.3	43.5	221.8	59.2	7.6
Standard deviation	117.4	30.7	103.4	37.8	5.6
Confidence levels (95.0%)	31.2	8.2	27.4	10.0	1.5
Coefficients of variation	0.324	0.642	0.438	0.531	0.765

P represents annual rainfall; P_1 represents rainfall in spring; P_2 represents rainfall in summer; P_3 represents rainfall in autumn; and P_4 represents rainfall in winter.

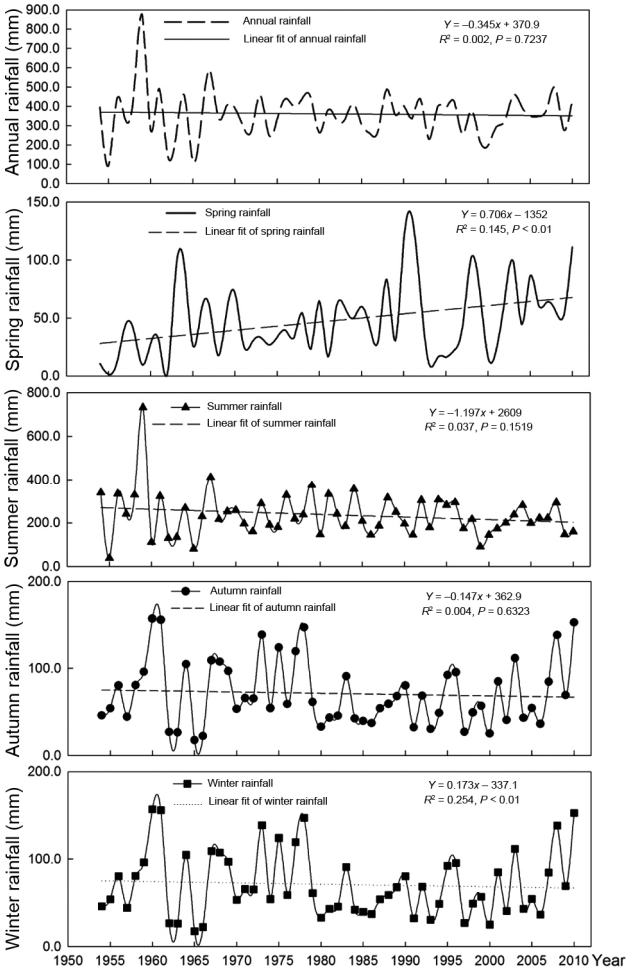

Figure 2. Mean annual and seasonal precipitation in the Huangfuchuan Watershed during 1954–2010.

The average precipitation in the study region during spring, summer, autumn, winter and the entire year was 47.9, 235.8, 71.1, 7.4 and 362.0 mm respectively (Table 1). The average precipitation during summer accounted for 65.1% of the average annual precipitation. The range between the minimum and maximum values for each variable was quite large. The coefficients of variation (CVs) for the seasonal precipitation ranged from 0.438 (in summer) to 0.765 (in winter), implying unstable changes. From 1954 to 2010, the average spring precipitation and average winter precipitation significantly increased with linear trends, while precipitation in the other seasons and the annual precipitation exhibited no significant trends as can be seen in Figure 2.

The figure thus presents the observed annual and seasonal precipitation during 1954–2010 in the study area. Table 2 provides the corresponding results of the MK tests. During the study period, there was a decrease in precipitation for summer, autumn and the entire year. The average annual decrease rates were –1.197, –0.147 and –0.345 mm/a respectively. Precipitation in spring and winter showed a significantly increase trend. The average annual rates of increase were 0.706 and 0.173 mm/a respectively.

There were no abrupt changes in annual precipitation, while they were detected for all four seasons (Table 3). The abrupt change of precipitation in summer occurred during 1986–1994, which is similar to the results of Ding *et al.*[24] for east China and those of Su *et al.*[25] in the Yangtze River basin. Furthermore, abrupt changes within the range 1963–1998 were consistent with annual precipitation found in the Yellow River basin[26].

By employing the EEMD technique, the original annual and seasonal rainfall time series were decomposed into one residue and four independent IMFs respectively. Figure 3 *a–e* shows results of this process for the seasonal and annual precipitation. It can be observed that precipitation data are decomposed into IMFs. It can also be seen that the IMFs present various wavelengths, frequencies and amplitudes. IMF1 exhibits the shortest wavelength, maximum amplitude and highest frequency. The IMF components increase in wavelength and decrease in amplitude and frequency as their rank increases. The residue (RES) represents a mode that is slowly varying about the long-term average.

Within the EEMD method, each IMF component captures fluctuation characteristics at different timescales from high to low frequency, and the residue component reflects the original data trend over time. In general, each

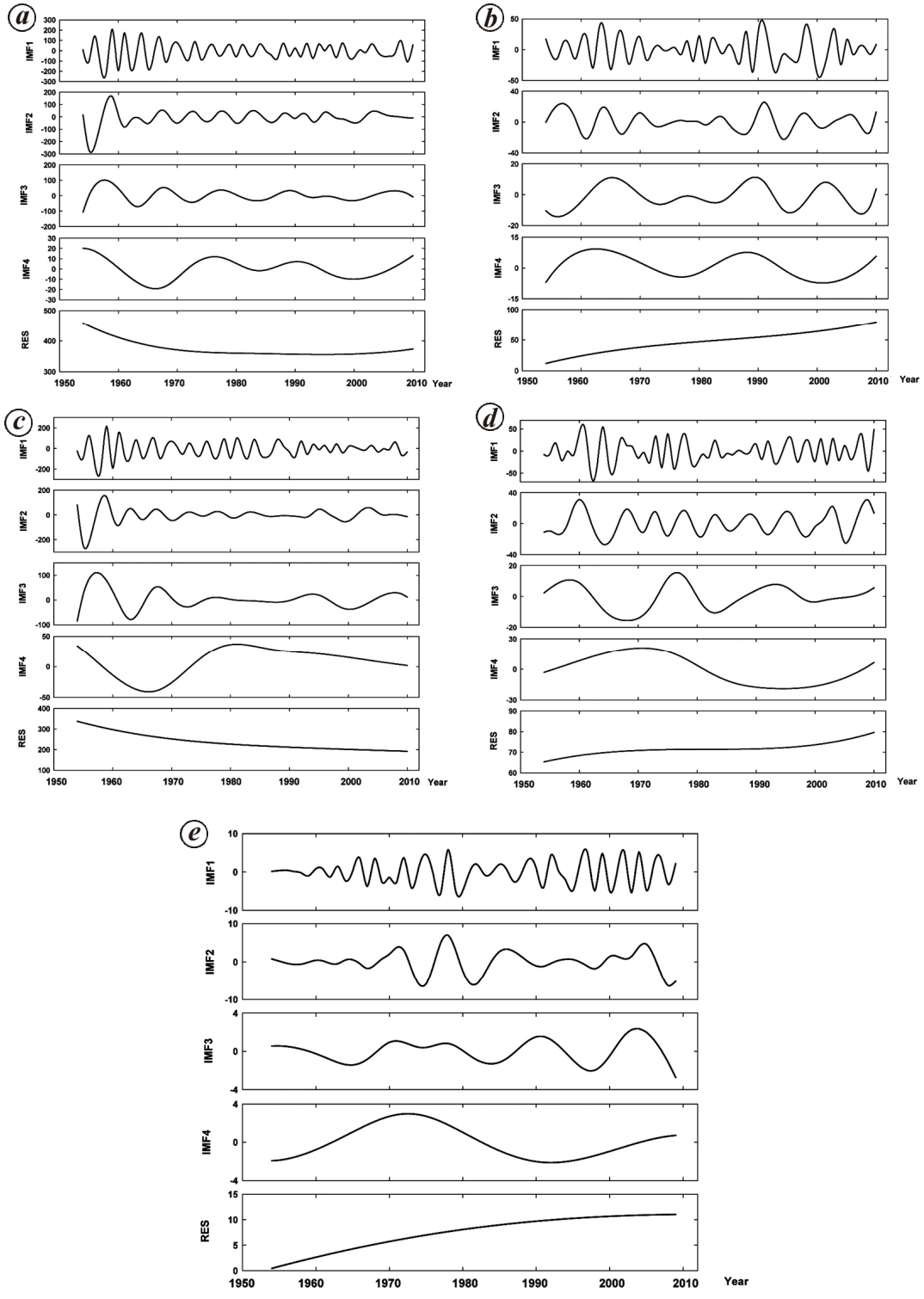

Figure 3 ***a–e***. Ensemble empirical mode decomposition of (***a***) annual precipitation time series, (***b***) spring precipitation time series, (***c***) summer precipitation time series, (***d***) autumn precipitation time series and (***e***) winter precipitation time series from 1954 to 2010.

IMF component captures the oscillation in the original series of inherently different characteristic scales. The physical meaning contained in IMF components can be determined by significance testing, and different significance levels reflect the robustness of the physical interpretation.

Table 2. Trend analysis for annual and seasonal precipitation during 1954–2010 in the Huangfuchuan Watershed

Variable	Mann–Kendall	
	Z statistic	Significance level
Annual precipitation	–0.18	–
Spring precipitation	2.96*	0.01
Summer precipitation	–1.25	–
Autumn precipitation	–0.39	–
Winter precipitation	4.65*	0.01

*Represents significance at the $P = 0.01$ level.

Table 4 clearly shows that IMF4 (quasi-52-year cycle) of precipitation in autumn as well as IMF2 (quasi-6-year cycle) and IMF4 (quasi-48-year cycle) of precipitation in winter are significant at the $P = 0.05$ level. This suggests that these IMFs are relatively more important and reflect more physically meaningful information. It should be noted that although there is less physically meaningful information contained in most of IMFs, they are still involved in our calculation for the variance contribution rate to maintain the total energy of the signal (Table 4). Taking the spring precipitation as an example, when connecting Figure 3 *b* and Table 4, the IMF1 contribution to precipitation variance in the quasi-3-year is greatest and approaches 31.40%. The amplitude of the precipitation oscillates strongly within a decrease–increase–decrease trend and is markedly higher in the early 1960s and late 1990s. The IMF2 component contributes approximately 25.50% to the precipitation variance of the quasi-6-year cycle, indicating higher precipitation levels in the early 1960s and early 1990s. The IMF3 component contributes 21.10% to the quasi-12-year precipitation variance, which indicates a relatively larger amplitude in the early 1960s and late 1990s. The IMF4 component contributes 13.90% to the precipitation variance of the quasi-25-year cycle, which indicates that the precipitation amplitude and instability of variation rise at this timescale. The trend components contribute up to 8.10% towards the variance, which indicates that the overall average annual spring precipitation in the Huangfuchuan Watershed during 1954–2010 exhibits a nonlinear increase as precipitation increases.

In this study, we utilized the EEMD statistical method to investigate periodicities in the precipitation of the Huangfuchuan Watershed in the Loess Plateau. Although the EEMD method can reveal the characteristics of internal changes in precipitation, it is not sufficient for mechanism analysis. Similar research also showed that although some IMFs contained less information with actual physical meaning, they are also involved in the calculation of the variance contribution rate in maintaining the total energy of the signal[27]. In addition, the IMFs extracted by EEMD may not be authentic due to the addition of white noise sequence suggested by Wu and Huang[21]. In this study, the variance contribution of the first two IMFs accounted for more than 50% of the total variance. This indicates high-frequency characteristics in both annual and seasonal precipitation. However, only a few IMFs passed the significance tests, and most of the information in the IMFs was white noise[28]. This further indicates that there were only quasi-52-year cycles of precipitation in autumn as well as quasi-6-year cycles and quasi-48-year cycles of precipitation in winter in the study area.

The period of precipitation in autumn was quasi-3-, quasi-5-, quasi-14-, and quasi-52-year. This is consistent with the study of Xue *et al.*[3], who autumn rainfall in high-frequency modes in Weihe River Basin. The period of precipitation in spring was quasi-3-, quasi-6-, quasi-11-, and quasi-25-year; and in summer the periods were quasi-3-, quasi-5-, quasi-10-, and quasi-50-year. These results are in agreement with those of Deng *et al.*[4] for spring and summer rainfall in high-frequency modes in the Yangtze River Basin. The IMF1 and IMF2 components of seasonal precipitation levels in Table 2 illustrate that there is noticeable periodic variability within 3 years and 5–6 years respectively. According to multiple timescale analysis of sea surface temperature (SST) data over the last 100 years[29], there is also obvious periodic variability within 3–4 and 6–8 years. Hence the high-frequency components of the seasonal rainfall series are consistent with SST and demonstrate that the short-term variation in the study area may be affected by SST. The observed temporal variability in seasonal rainfall may be explained by periodicities associated with the North Atlantic Oscillation and the Atlantic Multidecadal Oscillation.

Table 5 shows the Hurst indices based on the annual and seasonal precipitation time series from 1954 to 2010. The *H* value for annual precipitation was 0.49, while for seasonal precipitation levels it ranged from a minimum of 0.53 (in summer) to a maximum of 0.77 (in winter). An *H* value which is greater than 0.50 indicates that the future trend should be similar to the past trend, with a greater value suggesting a greater likelihood of persistence. Therefore, the results suggest persistence in the long-term trends of seasonal precipitation. These results are in agreement with those of Li *et al.*[2], in a study conducted in Xinjiang, China.

Thus the analysis of the trends, abrupt changes and periodic variabilities of annual and seasonal precipitation in the Huangfuchuan Watershed provides the following conclusions.

The MK test results indicate the occurrence of abrupt precipitation change in all four seasons. The abrupt change years ranged from 1962 to 1994. There were abrupt changes during spring in 1963–1969 and 1975, during summer in 1962 and 1986–1994, during autumn in 1978, and during winter in 1964. The annual precipitation exhibited no abrupt change.

The annual and seasonal precipitation levels in the Huangfuchuan Watershed are subject to quasi-3-year and

Table 3. Abrupt change in annual and seasonal precipitation during 1954–2010 in the Huangfuchuan Watershed

Annual/seasonal	Annual	Spring	Summer	Autumn	Winter
Year	–	(1963–1969)* and 1975*	1962* and (1986–1994)*	1978*	1964*

*Represents significance at the $P = 0.05$ level.

Table 4. The mean periods of various timescale components obtained by ensemble empirical mode decomposition for annual and seasonal precipitation during 1954–2010 in the Huangfuchuan Watershed

Annual/seasonal	Variable	IMF1	IMF2	IMF3	IMF4	RES
Annual	Period (yrs)	2.7	5.2	8.1	19.2	
	Contribution (%)	32.00	23.10	19.80	13.50	11.60
Spring	Period (yrs)	3.0	5.7	11.4	24.8	
	Contribution (%)	31.40	25.50	21.10	13.90	8.10
Summer	Period (yrs)	2.7	5.2	9.5	49.7	
	Contribution (%)	29.20	22.00	20.80	17.90	10.10
Autumn	Period (yrs)	2.6	5.2	14.3	51.6*	
	Contribution (%)	30.10	23.20	21.00	15.70	10.00
Winter	Period (yrs)	3.0	6.2*	9.3	47.8*	
	Contribution (%)	28.40	23.10	19.40	17.80	11.30

*Represents significance at the $P = 0.05$ level.

Table 5. *R*/*S* analysis for annual and seasonal patterns during 1954–2010 in the Huangfuchuan Watershed

R/*S* analysis	Annual	Spring	Summer	Autumn	Winter
H value	0.49	0.58	0.53	0.75	0.77

quasi-6-year interannual periodical features according to the EEMD analysis, whereas decadal periods are dominated by quasi-9-year and quasi-49-year periods. However, the interannual periodicity is not statistically significant. The IMF4 (quasi-52-year cycle) of precipitation in autumn as well as the IMF2 (quasi-6-year cycle) and IMF4 (quasi-48-year cycle) of precipitation in winter are statistically significant at the $P = 0.05$ level. This suggests that these IMFs are important components that contain more physically meaningful information. The other IMFs are not statistically significant, which suggests that they contain less physically meaningful information. Further studies are required to explain the relationships between these precipitation periodicities and the climatic factors.

The Hurst exponent analysis indicates that the *H* value is greater than 0.50 for all four seasons and less than 0.50 for annual precipitation. This means that the current trends of seasonal precipitation will continue in the future.

1. Coulibaly, P., Spatial and temporal variability of Canadian seasonal precipitation (1900–2000). *Adv. Water Resour.*, 2006, **29**, 1846–1865.
2. Li, Q. H., Chen, Y. N., Shen, Y. J., Li, X. G. and Xu, J. H., Spatial and temporal trends of climate change in Xinjiang, China. *J. Geogr. Sci.*, 2011, **21**, 1007–1018.
3. Xue, C. F., Hou, W., Zhao, J. H. and Wang, S. G., The application of ensemble empirical mode decomposition method in multiscale analysis of region precipitation and its response to the climate change. *Acta Phys. Sin.*, 2013, **62**, 109203-1–109203-8.
4. Deng, H. Q., Luo, Y., Yao, Y. and Liu, C., Spring and summer precipitation changes from 1880 to 2011 and the future projections from CMIP5 models in the Yangtze River Basin, China. *Quaternary Int.*, 2013, **304**, 95–106.
5. Padmanabhan, G. and Rao, A. R., Maximum entropy spectral analysis of hydrologic data. *Water Resour. Res.*, 1988, **24**, 1519–1533.
6. Dalezios, N. R. and Tyraskis, P. A., Maximum entropy spectra for regional precipitation analysis and forecasting. *J. Hydrol.*, 1989, **109**, 25–42.
7. He, Y., Mu, X. M., Gao, P., Zhao, G. J., Wang, F., Sun, W. Y. and Zhang, Y. Q., Spatial variability and periodicity of precipitation in the middle reaches of the Yellow River, China. *Adv. Meteorol.*, 2016, **2016**, 1–9.
8. Kennett, B. L. N. and Engdahl, E. R., Traveltimes for global earthquake location and phase identification. *Geophys. J. Int.*, 1991, **105**, 429–465.
9. Cruz, R. V. and Góes, L. C. S., Results of short-period helicopter system identification using output-error and hybrid search-gradient optimization algorithm. *Math. Probl. Eng.*, 2010, **2010**, 1–17.
10. Lima, C. H. R. and Lall, U., Spatial scaling in a changing climate: a hierarchical Bayesian model for non-stationary multi-site annual maximum and monthly streamflow. *J. Hydrol.*, 2010, **383**, 307–318.
11. Franzke, C., Nonlinear trends, long-range dependence, and climate noise properties of surface temperature. *J. Climate*, 2012, **25**, 4172–4183.
12. Shi, F., Yang, B., Gunten, L., Qin, C. and Wang, Z. Y., Ensemble empirical mode decomposition for tree-ring climate reconstructions. *Theor. Appl. Climatol.*, 2012, **109**, 233–243.
13. Qian, C., Fu, C. B., Wu, Z. H. and Yan, Z. W., On the secular change of spring onset at Stockholm. *Geophys. Res. Lett.*, 2009, **36**, L12706.
14. Li, E. H., Mu, X. M., Zhao, G. J., Gao, P. and Shao, H. B., Variation of runoff and precipitation in the Hekou–Longmen region of

the Yellow River based on elasticity analysis. *Sci. World J.*, 2014, **2014**, 1–11.
15. Mann, H. B., Nonparametric tests against trend. *Econometrica*, 1945, **13**, 245–259.
16. Kendall, M. G., *Rank Correlation Methods*, Griffin, London, UK, 1975.
17. Zhang, Q., Xu, C. Y., Becker, S., Zhang, Z. X., Chen, Y. D. and Coulibaly, M., Trends and abrupt changes of precipitation maxima in the Pearl River basin, China. *Atmos. Sci. Lett.*, 2009, **10**, 132–144.
18. Wu, Z. H., Huang, N. E. and Chen, X. Y., The multi-dimensional ensemble empirical mode decomposition method. *Adv. Adapt. Data Anal.*, 2009, **1**, 339–372.
19. Huang, N. E. *et al.*, The empirical mode decomposition and the Hilbert spectrum for nonlinear and non-stationary time series analysis. *Proc. Math., Phys. Eng. Sci.*, 1998, **454**, 903–995.
20. Huang, N. E. and Wu, Z. H., A review on Hilbert–Huang transform: method and its applications to geophysical studies. *Rev. Geophys.*, 2008, **46**, RG2006.
21. Wu, Z. H. and Huang, N. E., Ensemble empirical mode decomposition: a noise-assisted data analysis method. *Adv. Adapt. Data Anal.*, 2009, **1**, 1–49.
22. Rehman, S., Study of Saudi Arabian climatic conditions using Hurst exponent and climatic predictability index. *Chaos Soliton. Fract.*, 2009, **39**, 499–509.
23. Sakalauskiene, G., The Hurst phenomenon in hydrology. *Environ. Res. Eng. Manage.*, 2003, **3**, 16–20.
24. Ding, Y. H., Wang, Z. Y. and Sun, Y., Inter-decadal variation of the summer precipitation in East China and its association with decreasing Asian summer monsoon. Part I: Observed evidences. *Int. J. Climatol.*, 2008, **28**, 1139–1161.
25. Su, B. D., Jiang, T., Shi, Y. F., Stefan, B. and Marco, G., Observed precipitation trends in the Yangtze river catchment from 1951 to 2002. *J. Geogr. Sci.*, 2004, **14**, 204–218.
26. Liu, Q., Yang, Z. F. and Ćui, B. S., Spatial and temporal variability of annual precipitation during 1961–2006 in Yellow River Basin, China. *J. Hydrol.*, 2008, **361**, 330–338.
27. Bai, L., Xu, J. H., Chen, Z. S., Li, W. H., Liu, Z. H., Zhao, B. F. and Wang, Z. J., The regional features of temperature variation trends over Xinjiang in China by the ensemble empirical mode decomposition method. *Int. J. Climatol.*, 2015, **35**, 3229–3237.
28. Wu, Z. H. and Huang, N. E., A study of the characteristics of white noise using the empirical mode decomposition method. *Proc. R. Soc. London, Ser. A.*, 2004, **460**, 1597–1611.
29. Sun, X. and Lin, Z. S., A new technology HHT and its diagnosis for ENSO. *Meteorol. Mon.*, 2006, **32**, 17–22.

ACKNOWLEDGEMENTS. This research was supported by the Non-profit Industry Financial Program of MWR, China (201501049), West Light Foundation and Youth Innovation Promotion Association, Chinese Academy of Sciences (2011289), the Hundred Talents Project of the Chinese Academy of Sciences (A315021406), Program for Key Science and Technology Innovation Team in Shaanxi Province (2014KCT-27), the Natural Science Foundation of Shaanxi Province (2015JQ4112) and the Key Research Program of the Chinese Academy of Sciences [KZZD-EW-04].

Received 14 December 2015; revised accepted 14 February 2016

doi: 10.18520/cs/v111/i4/727-733

Predatory stress paradigm to induce anxiety-like behaviour in juvenile male C57BL/6J mice

Abraão Tiago Batista Guimarães[1], Joyce Moreira de Souza[1], Wellington Alves Mizael da Silva[1], Bruna de Oliveira Mendes[2], Joice Gomes de Queiroz[2], André Luis da Silva Castro[1,3] and Guilherme Malafaia[1,2,4,*]

[1]Programa de Pós-Graduação em Conservação de Recursos Naturais do Cerrado, and
[2]Laboratório de Pesquisas Biológicas, and
[3]Laboratório de Zoologia, Instituto Federal Goiano – Câmpus Urutaí, GO, Brazil
[4]Programa de Pós-Graduação em Biodiversidade Animal, Universidade Federal de Goiás – Câmpus Samambaia, Goiânia, Brazil

The present study deals with a chronic stress paradigm to induce anxiety-like behaviour in male C57Bl/6J mice, using Wistar rats as predators. The predatory stress paradigm includes placing the mice in a cage protected by a metallic screen, which is placed inside a larger metallic cage, containing adult male Wistar rats. Male mice (21 days old) were put in indirect contact with Wistar male rats for 1 h daily for 12 days. The anxiety behaviour of mice was analysed by means of elevated plus-maze test, after 12 days of predatory stress daily (first behavioural assessment) and 12 days after the stress protocol (second behavioural assessment). We demonstrate that this predatory stress paradigm induces anxiety-like behaviour in male juvenile mice C57Bl/6J. We conclude that the predatory stress paradigm used is capable of inducing anxiety in male C57Bl/6J mice after a short duration (12 days) of predatory stress with Wistar rats.

Keywords: Anxiety, elevated plus maze test, juvenile mice, predatory stress.

ONE of the psychiatric disorders associated with the damaging effects of stress is anxiety. Unfortunately, we know very little about how the changes in stress load with time are related to changes in anxiety prodromal symptoms and to the development of an anxiogenic disorder[1]. In order to understand the ethology of anxiety and its relationship with stress and stressors, laboratory animals have been used in different studies, whereby a probable situation suffered in various forms of discomfort. As noted by Nunes and Hallak[2], these studies provide important inputs for the treatment of stress and its effects.

*For correspondence. (e-mail: guilhermeifgoiano@gmail.com)